Applied Surface Science 327 (2015) 213–217

Contents lists available at ScienceDirect

Applied Surface Science

journal homepage: www.elsevier.com/locate/apsusc

Synthesis of semimetal A_3Bi (A = Na, K) thin films by molecular beam epitaxy

Jing Wen[a,*], Hua Guo[a], Chen-Hui Yan[a,b], Zhen-Yu Wang[a], Kai Chang[a], Peng Deng[a], Teng Zhang[a], Zhi-Dong Zhang[b], Shuai-Hua Ji[a], Li-Li Wang[c], Ke He[c], Xu-Cun Ma[c], Xi Chen[a], Qi-Kun Xue[a,*]

[a] State Key Laboratory of Low-Dimensional Quantum Physics, Department of Physics, Tsinghua University, Beijing 100084, China
[b] Shenyang National Laboratory for Materials Science, Institute of Metal Research, Chinese Academy of Sciences, Shenyang 110016, China
[c] Institute of Physics, Chinese Academy of Sciences, Beijing 100190, China

ARTICLE INFO

Article history:
Received 14 October 2013
Received in revised form 30 October 2014
Accepted 16 November 2014
Available online 22 November 2014

Keywords:
Na_3Bi
K_3Bi
STM
ARPES
MBE

ABSTRACT

Three-dimensional (3D) Dirac cones are predicted to reside in semimetals A_3Bi (A = Na, K). By using molecular beam epitaxy (MBE) and scanning tunneling microscopy (STM), we have successfully established the growth conditions for Na_3Bi thin films on Si(1 1 1)-7 × 7, and determined that the lattice of Na_3Bi is rotated by 30 degree with respect to that of Si(1 1 1)-7 × 7. The Na_3Bi/Si(1 1 1)-7 × 7 thin film was further used as the substrate for the growth of K_3Bi. The 3D Dirac-cone-like electronic band structures of Na_3Bi and K_3Bi have been clearly revealed by angle resolved photoelectron spectroscopy (ARPES).

1. Introduction

The discovery of Dirac-like band structure in graphene has led to significant attention partially due to its potential to simulate high energy physics with condensed matter [1–5]. In the presence of spin–orbit coupling as well as time-reversal symmetry, the Dirac-cone structure in momentum space can also be found in topological insulators [6–8,3,9–15], such as Bi_2Se_3, Bi_2Te_3, and Sb_2Te_3 [16–20]. Although with a different origin, their surface states mimic the band structure of graphene to a large extent. In addition, the surface states are protected by time-reversal symmetry and are immune to backscattering. The search for new generation of Dirac-cone-like band structure in other systems can provide us with new physics and potential applications. Recently, it has been proposed that a new kind of topological material called topological semimetal, such as Na_3Bi and K_3Bi, may also harbor a Dirac-cone-like structure, which is directly linked to the presence of crystal symmetry [21–23]. The Dirac cones in these materials are three-dimensional, unlike the two-dimensional surface states in topological insulators. The three-dimensional Dirac cone allows for novel realization of high-energy phenomena in condensed matter physics as well as possible applications in spintronics. In this paper, we report the growth of Na_3Bi and K_3Bi by MBE and their electronic band structures revealed by ARPES.

2. Experimental methods

The bulk crystals of Na_3Bi and K_3Bi are difficult to handle because of their high chemical reactivity in air. Therefore we attempt to grow thin films in ultra-high vacuum and measure their electronic structures *in situ*. The experiments were carried out on an Omicron MBE-STM-ARPES combined system in ultra-high vacuum with a base pressure better than 1×10^{-10} mbar. Si(1 1 1)-7 × 7 substrates were cleaned by a standard multi-cycle flashing process. Sodium was bought from Alfa Aesar with a purity of 99.95% and bismuth was from NILACO Co. with a purity of 99.999%. The growth dynamics of Na_3Bi is similar to that of Bi_2Se_3 and Bi_2Te_3 [20,26–29]. Sodium and bismuth from two Knudsen cells held at 190° and 495°, respectively, were evaporated onto the Si(1 1 1)-7 × 7 substrate, which is maintained at 250–300°. The growth proceeds under Na-rich condition (Na/Bi flux ratio = 10–20) and the growth rate only depends on the Bi flux. The extra Na on the surface can quickly desorb under the above growth condition and does not incorporate into the film. Imaging of the samples was performed *in situ*

* Corresponding author. Tel.: +86 13426408186.
E-mail address: wenj07@126.com (J. Wen).

http://dx.doi.org/10.1016/j.apsusc.2014.11.083
0169-4332/

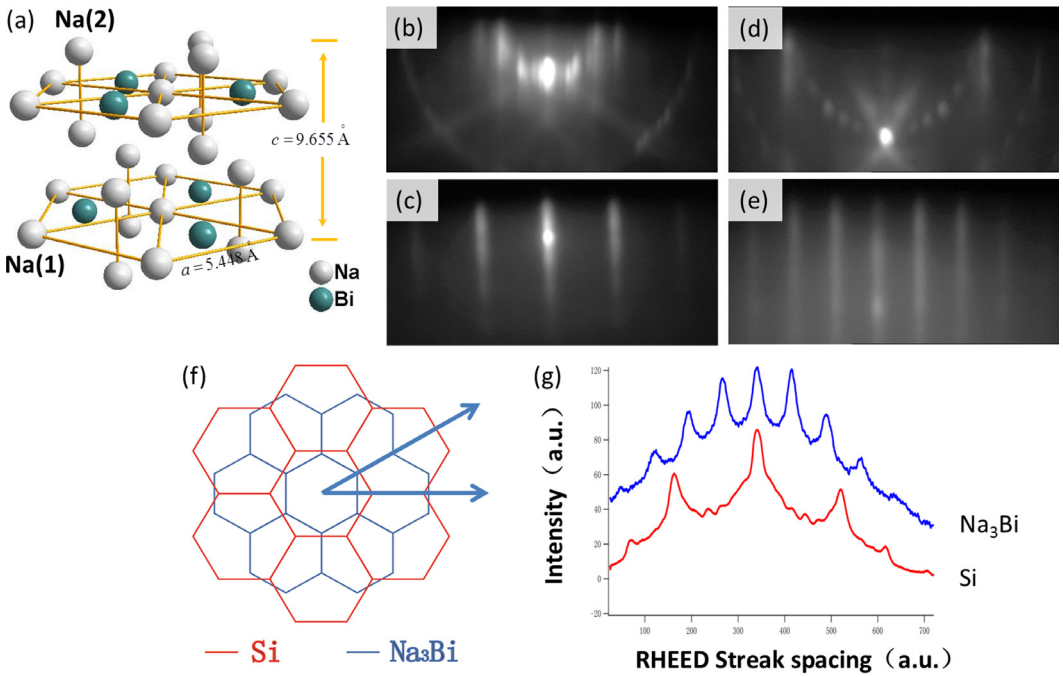

Fig. 1. (a) Crystal structure of Na_3Bi with $P6_3/mmc$ symmetry and two nonequivalent Na sites (Na(1), Na(2)). (b) RHEED pattern of the Si(1 1 1)-7 × 7 substrate along the $\langle 1\,1\,\bar{2} \rangle$ direction of Si(1 1 1) before growth. (c) RHEED pattern of Na_3Bi along the ⟨1 1 0⟩ direction of Na_3Bi(1 0 0) after growth. (d) RHEED pattern of Si(1 1 1)-7 × 7 along the ⟨1 1 0⟩ direction of Si(1 1 1) before growth. (e) RHEED pattern of Na_3Bi(1 0 0) along the $\langle 1\,1\,\bar{2} \rangle$ direction of Na_3Bi after growth. (f) Illustration of 30-degree rotation of reciprocal lattice of Na_3Bi and Si. (g) RHEED streak spacing of Na_3Bi(1 0 0) and Si(1 1 1).

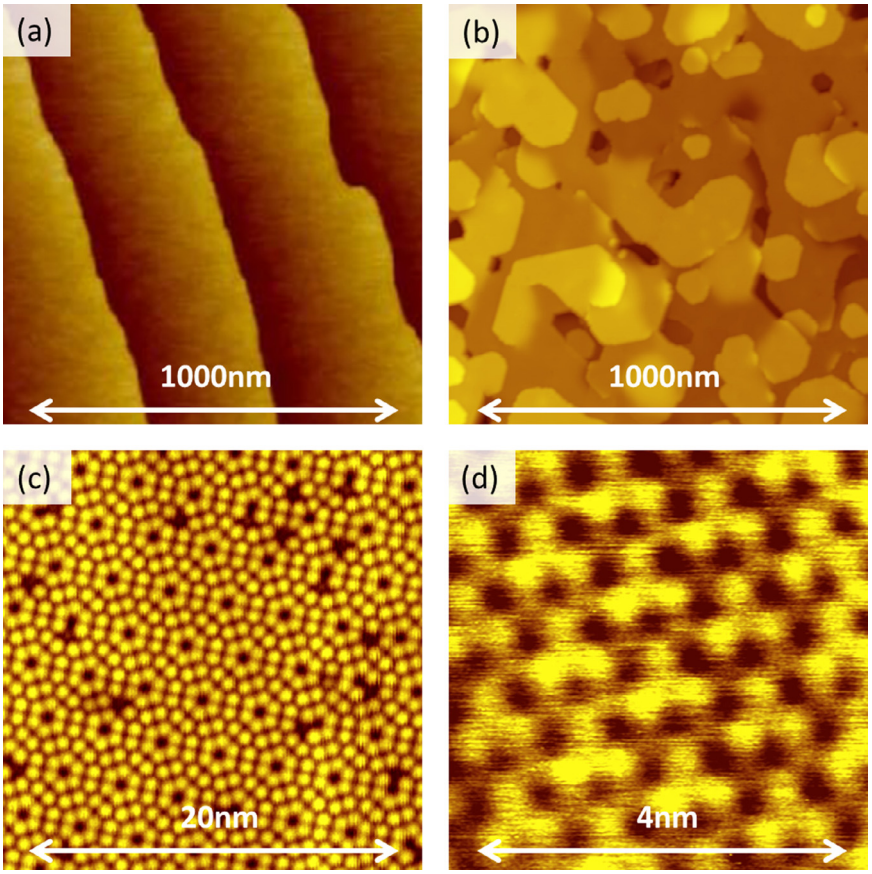

Fig. 2. STM images (1000 nm × 1000 nm), acquired from (a) the Si(1 1 1)-7 × 7 substrate and (b) the 20 nm-thick Na_3Bi(1 0 0) film. High-resolution images are (c) the Si(1 1 1)-7 × 7 substrate and (d) Na_3Bi(1 0 0).

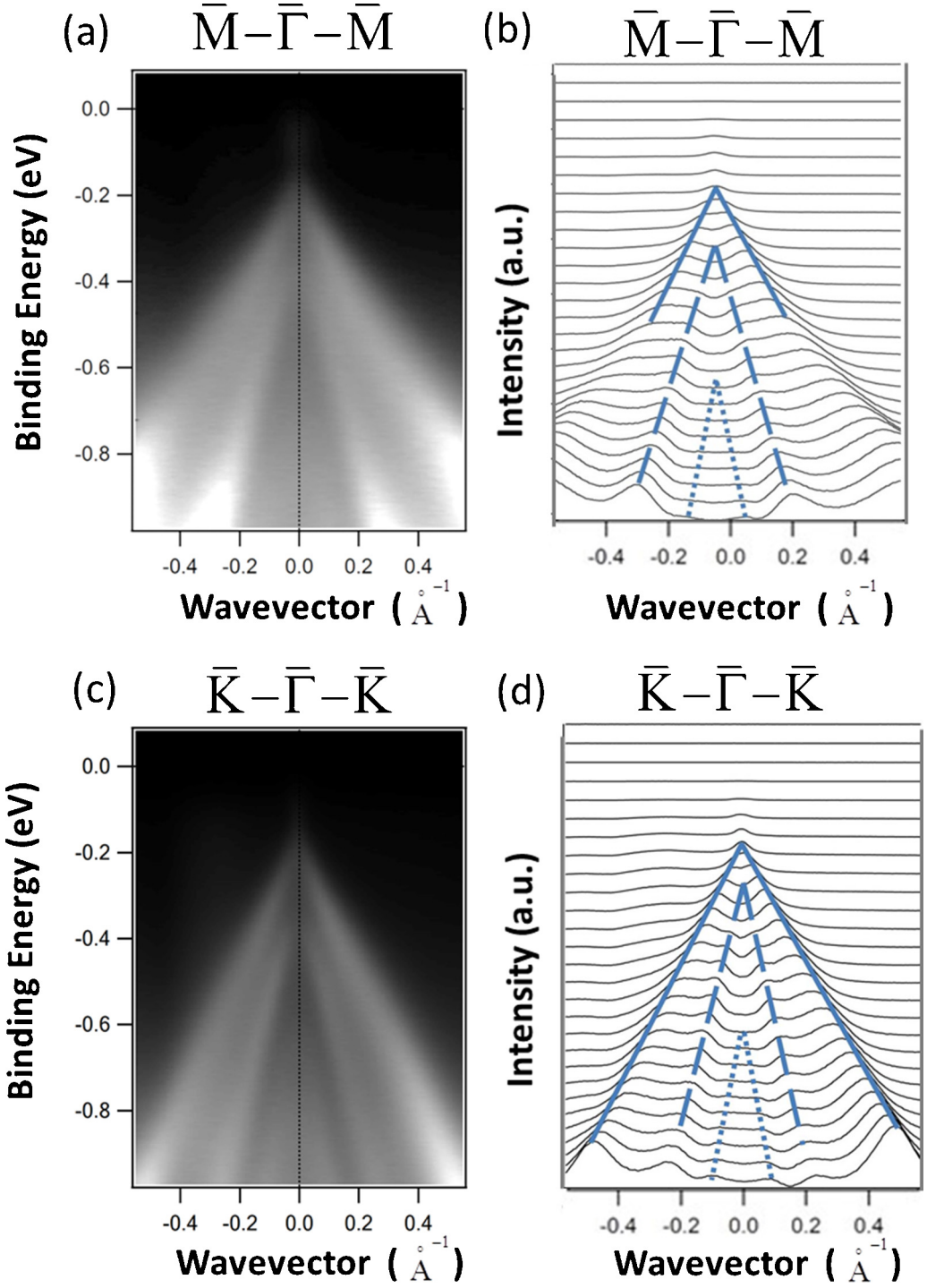

Fig. 3. ARPES measurements of the Na_3Bi film along (a) $\bar{\Gamma}-\bar{M}$ and (c) $\bar{\Gamma}-\bar{K}$ directions. The multi-cone structure is evident. The momentum distribution curves (MDCs) of ARPES results along (b) $\bar{\Gamma}-\bar{M}$ and (d) $\bar{\Gamma}-\bar{K}$ directions, fitting all the band structures. All bands fit well to linear correlation; however, the outer band along $\bar{\Gamma}-\bar{M}$ direction diverges from linear correlation at large wavevector.

using STM at liquid nitrogen temperature. The bias voltage was applied to the sample, while the tip was grounded. The ARPES spectra of Na_3Bi and K_3Bi were also collected at liquid nitrogen temperature with an R4000 analyzer and a VUV 5000 UV light source with a monochrometer. The He I alpha line (21.218 eV) was used. The energy and angular resolutions were 10 meV and 0.2 degree, respectively. The photoemission was measured at surface normal.

3. Results and discussion

Fig. 1 shows the crystal structure of Na_3Bi and the change of RHEED pattern before and after MBE growth. Na_3Bi and K_3Bi belong to alkali pnictides A_3Bi (A = Li, Na, K, Rb, Cs). Up until now, the physical properties of A_3Bi are not widely studied [24]. Although their chemical compositions are similar, A_3Bi belongs to two different space groups. Li_3Bi and Cs_3Bi have cubic $Fm\bar{3}m$ structure, while

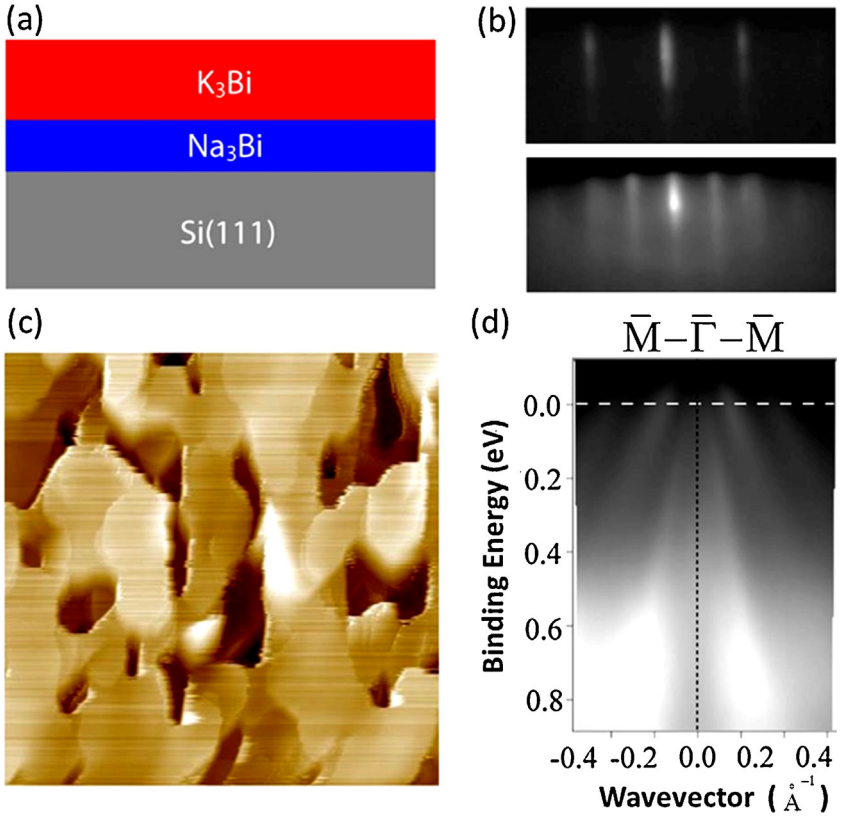

Fig. 4. (a) Illustration of K_3Bi grown on Na_3Bi/Si(1 1 1)-7 × 7. (b) RHEED of Na_3Bi/Si(1 1 1)-7 × 7 (above) and K_3Bi (below). (c) 200 nm × 200 nm STM image of a 20 nm-thick K_3Bi film. (d) ARPES measurement of K_3Bi along the $\bar{\Gamma} - \bar{M}$ direction.

Na_3Bi and K_3Bi are of hexagonal $P6_3/mmc$ structure [25]. The lattice of Na_3Bi has two nonequivalent Na sites, Na(1) and Na(2) in Fig. 1(a). Na(1) and Bi form the hexagonal layer, while Na(2) atoms reside in between two Na(1)–Bi layers and make connections to Bi atoms. The periods of Na(1) and Na(2) are both equal to the in-plane lattice constant of 5.448 Å, and the out-of-plane lattice constant is 9.655 Å as seen in Fig. 1(a).

The RHEED patterns of the Si substrate and the epitaxial Na_3Bi(0 0 1) film were shown in Fig. 1(b)–(e). The direction of incident electron beam and the substrate position are fixed. If the lattice vectors of Si(1 1 1) before MBE growth and Na_3Bi(0 0 1) after growth coincide, we should see RHEED patterns along the same direction. However, we observe that if the incident electron beam is along the ⟨1 1 0⟩ direction of Si(1 1 1) before growth, then the RHEED pattern is obtained along $\langle 1\,1\,\bar{2} \rangle$ of the Na_3Bi film after growth. This result suggests that the base vectors of the Na_3Bi lattice rotate by 30 degree with respect to those of Si, as illustrated in Fig. 1(f). To further confirm this result, we aligned the incident electron beam along the $\langle 1\,1\,\bar{2} \rangle$ direction of the Si substrate, and after growth, the RHEED pattern changed to along the ⟨1 1 0⟩ direction of the Na_3Bi film.

We also calibrated the in-plane lattice constant of the Na_3Bi film with respect to the Si(1 1 1)-7 × 7 surface by RHEED patterns in Fig. 1(g). According to the RHEED streaks, the Na_3Bi film has a hexagonal structure and the in-plane lattice constant is found to be 5.46 Å. The RHEED intensity of (0,0) diffraction was recorded by a CCD camera to monitor its change during the growth process. No intensity oscillation is observed during growth, suggesting that the growth of Na_3Bi on Si(1 1 1)-7 × 7 might not follow 2D growth mode.

A typical STM image of a 20 nm-thick Na_3Bi(1 0 0) film is shown in Fig. 2(b). Na_3Bi is a layered material and its interaction with the underlying Si substrate is relatively weak. The atomically flat surface is immediately evident. Spiral and line dislocations can be seen in the image. The step height is 4.8 Å, corresponding to the half unit cell of Na_3Bi as seen in Fig. 1(a), which is the thickness of one Na(1)–Bi layer. The atomically resolved STM image of Na_3Bi shows the trimmer structure, as observed in Fig. 2(d), which is different from the close-pack configuration of Na-terminated surface. It indicates surface reconstruction and needs further investigation.

The Na_3Bi film has a hexagonal surface Brillouin zone (SBZ). Due to the closed shell configuration, Na_3Bi (K_3Bi) is expected to be a semiconductor. However, band structure calculations reveal that Na_3Bi (K_3Bi) is a Dirac semimetal [21].

We carried out ARPES measurements along $\bar{\Gamma} - \bar{K}$ and $\bar{\Gamma} - \bar{M}$ directions. Fig. 3(a) and (c) shows the band structure of a 20 nm-thick Na_3Bi film observed near the $\bar{\Gamma}$ point along the two high-symmetry directions. Within a narrow binding-energy window below the Fermi level E_F, three cone-shaped bands are observed in both directions. The apexes of the cones do not overlap at a single point. The momentum distribution curve (MDC) is defined as the ARPES intensity as a function of wavevector at a constant binding energy. By fitting the band in MDCs, as seen in Fig. 3(b) and (d), we observe that the outer band fit perfectly to line along the $\bar{\Gamma} - \bar{K}$ direction, but diverges from linear correlation along the $\bar{\Gamma} - \bar{M}$ direction. This is similar to the warping effect of surface band of topological insulator [6]. Because the photon energy is not tunable in the current experiment, it is still difficult to compare the ARPES data with the three-dimensional Dirac cone structure given by calculation.

Furthermore, we also tried to grow K_3Bi on Si(1 1 1)-7 × 7 substrate. We used K source from Alfa Aesar with a purity of 99.95%, while Bi source was the same as for Na_3Bi. The identical MBE growth procedure of Na_3Bi was applied to K_3Bi, which was, $T_{Bi} > T_{substrate} > T_K$ and K-rich condition. But K atom is much more reactive than Na atom, as a result, the quality of the K_3Bi film grown

on Si(1 1 1)-7 × 7 is very poor in our experiment. In order to improve the quality of the K_3Bi film, we choose Na_3Bi/Si(1 1 1) as the substrate, since it is less reactive to K and has the better lattice match. In the experiment, a 20 nm Na_3Bi film was first deposited on Si(1 1 1)-7 × 7, then Bi and K were deposited on Na_3Bi/Si(1 1 1) to form a 20 nm-thick K_3Bi film as illustrated in Fig. 4(a), with $T_{Bi} = 495^\circ$, $T_K = 170^\circ$, $T_{substrate} = 230–270^\circ$, and Na/Bi flux ratio = 10–20. According to RHEED results in Fig. 4(b), the film has a hexagonal structure and the in-plain lattice constant is 6.15 Å. Further STM results confirm the RHEED results and directly reveal that the K_3Bi film has a flat surface and spiral dislocations, as seen in Fig. 4(c). We carried the ARPES experiment through the $\bar{\Gamma} - \bar{M}$ direction (Fig. 4(d)). The results show that K_3Bi also has multi-cone-shape band structures and all of them do not coincide in one point.

4. Summary

To summarize, we have established the growth dynamics and temperature criterion for MBE synthesis of Na_3Bi and K_3Bi films. Combined with ARPES measurements and STM imaging, the band structure and surface topography of the films are revealed. The work paves a material foundation for future study of the topological surface state of the films.

Acknowledgments

This work was financially supported by National Natural Science Foundation of China (Grant Nos. 11025419 and 50831006) and Ministry of Science and Technology of China (Grant No. 2011CB921904). We thank Z. Fang, X. Dai, and H. M. Weng for discussions.

References

[1] K.S. Novoselov, A.K. Geim, S.V. Morozov, D. Jiang, M.I. Katsnelson, I.V. Grigorieva, S.V. Dubonos, A.A. Firsov, Nature 438 (2005) 197.
[2] Y.B. Zhang, Y.W. Tan, H.L. Stormer, P. Kim, Nature 438 (2005) 201.
[3] C.L. Kane, E.J. Mele, Phys. Rev. Lett. 95 (2005) 226801.
[4] A.K. Geim, A.H. Macdonald, Phys. Today 60 (2007) 35.
[5] A.H. Castro Neto, F. Guinea, N.M.R. Peres, K.S. Novoselov, A.K. Geim, Rev. Mod. Phys. 81 (2009) 109.
[6] M.Z. Hasan, C.L. Kane, Rev. Mod. Phys. 82 (2010) 3045.
[7] X.L. Qi, S.C. Zhang, Rev. Mod. Phys. 83 (2011) 1057.
[8] S. Murakami, N. Nagaosa, S.C. Zhang, Science 301 (2003) 1348.
[9] B.A. Bernevig, S.C. Zhang, Phys. Rev. Lett. 96 (2006) 106802.
[10] S. Murakami, Phys. Rev. Lett. 97 (2006) 236805.
[11] B.A. Bernevig, T.L. Hughes, S.C. Zhang, Science 314 (2006) 1757.
[12] L. Fu, C.L. Kane, E.J. Mele, Phys. Rev. Lett. 98 (2007) 106803.
[13] J.E. Moore, L. Balents, Phys. Rev. B 75 (2007) 121306.
[14] X. Dai, T.L. Hughes, X.L. Qi, Z. Fang, S.C. Zhang, Phys. Rev. B 77 (2008) 125319.
[15] L. Fu, C.L. Kane, Phys. Rev. B 76 (2007) 045302.
[16] D. Hsieh, D. Qian, L. Wray, Y. Xia, Y.S. Hor, R.J. Cava, M.Z. Hasan, Nature 452 (2008) 970.
[17] Y.L. Chen, J.G. Analytis, J.-H. Chu, Z.K. Liu, S.-K. Mo, X.L. Qi, H.J. Zhang, D.H. Lu, X. Dai, Z. Fang, S.C. Zhang, I.R. Fisher, Z. Hussain, Z.X. Shen, Science 325 (2009) 178.
[18] Y. Xia, D. Qian, D. Hsieh, L. Wray, A. Pal, H. Lin, A. Bansil, D. Grauer, Y.S. Hor, R.J. Cava, M.Z. Hasan, Nat. Phys. 5 (2009) 398.
[19] H. Zhang, C.X. Liu, X.L. Qi, X. Dai, Z. Fang, S.C. Zhang, Nat. Phys. 5 (2009) 438.
[20] Y.Y. Li, G. Wang, X.G. Zhu, M.H. Liu, C. Ye, X. Chen, Y.Y. Wang, K. He, L.L. Wang, X.C. Ma, H.J. Zhang, Z. Fang, X.C. Xie, Y. Liu, X.L. Qi, J.F. Jia, S.C. Zhang, Q.K. Xue, Adv. Mater. 22 (2010) 4002.
[21] Z.J. Wang, Y. Sun, X.Q. Chen, C. Franchini, G. Xu, H.M. Weng, X. Dai, Z. Fang, Phys. Rev. B 85 (2012) 195320.
[22] T. Valla, H.W. Ji, L.M. Schoop, A.P. Weber, Z.H. Pan, J.T. Sadowski, E. Vescovo, A.V. Fedorov, A.N. Caruso, Q.D. Gibson, L. Muchler, C. Felser, R.J. Cava, Phys. Rev. B 86 (2012) 241101.
[23] K. Sun, W. Vincent Liu, A. Hemmerich, S. Das Sarma, Nat. Phys. 8 (2012) 67.
[24] M. Tegze, J. Hafner, J. Phys.: Condens. Matter 4 (1992) 2449.
[25] T.B. Massalski, Binary Alloy Phase Diagrams, ASM, Materials Park, 1990.
[26] Y. Zhang, K. He, C.Z. Chang, C.L. Song, L.L. Wang, X. Chen, J.F. Jia, Z. Fang, X. Dai, W.Y. Shan, S.Q. Shen, Q. Niu, X.L. Qi, S.C. Zhang, X.C. Ma, Q.K. Xue, Nat. Phys. 6 (2010) 584.
[27] Y. Zhang, C.Z. Chang, K. He, L.L. Wang, X. Chen, J.F. Jia, X.C. Ma, Q.K. Xue, Appl. Phys. Lett. 97 (2010) 194102.
[28] C.L. Song, Y.L. Wang, Y.P. Jiang, Y. Zhang, C.Z. Chang, L.L. Wang, K. He, X. Chen, J.F. Jia, Y.Y. Wang, Z. Fang, X. Dai, X.C. Xie, X.L. Qi, S.C. Zhang, Q.K. Xue, X.C. Ma, Appl. Phys. Lett. 97 (2010) 143118.
[29] G. Wang, X.G. Zhu, Y.Y. Sun, Y.Y. Li, T. Zhang, J. Wen, X. Chen, K. He, L.L. Wang, X.C. Ma, J.F. Jia, S.B. Zhang, Q.K. Xue, Adv. Mater. 23 (2011) 2929.